Cell Reports, Volume *28*

Supplemental Information

Mitochondrial GTP Links Nutrient Sensing to β Cell Health, Mitochondrial Morphology, and Insulin Secretion Independent of OxPhos

Sean R. Jesinkey, Anila K. Madiraju, Tiago C. Alves, OrLando H. Yarborough, Rebecca L. Cardone, Xiaojian Zhao, Yassmin Parsaei, Ali R. Nasiri, Gina Butrico, Xinran Liu, Anthony J. Molina, Austin M. Rountree, Adam S. Neal, Dane M. Wolf, John Sterpka, William M. Philbrick, Ian R. Sweet, Orian H. Shirihai, and Richard G. Kibbey

Supplemental Materials

Supplemental Figures

Supplemental Tables

Figure S1. Schematic depicting generation and transmission of the mtGTP signal to regulate glucose-stimulated insulin secretion in b-cells, and transient expression of hSCS-ATP and hSCS-GTP to modulate mtGTP in INS-1 832/13 cells, Related to Introduction and Figure 1

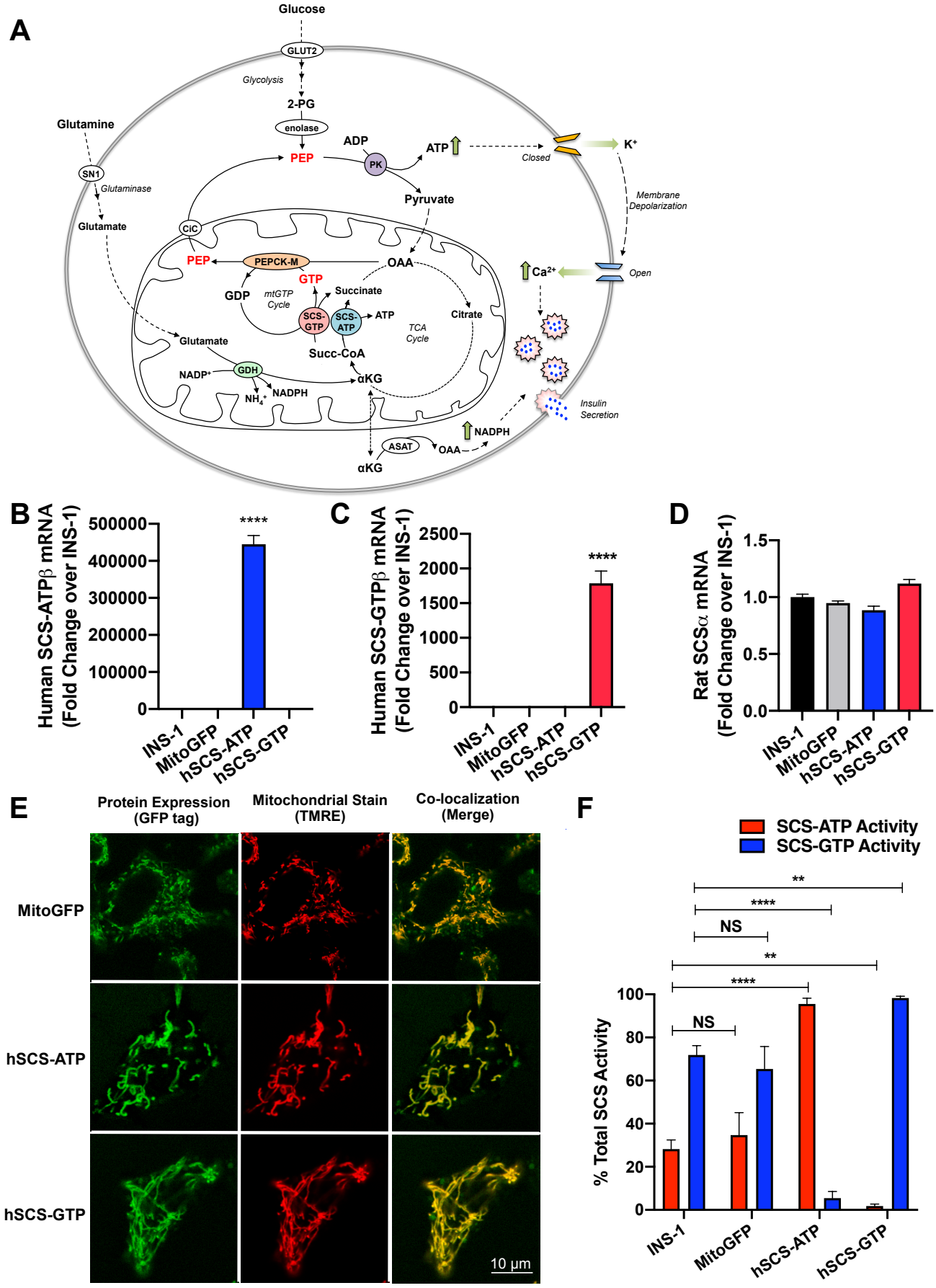

Figure S1 (A) Elevated circulating glucose increases glucose uptake via GLUT2 into the pancreatic β-cell. Glucose entering glycolysis is converted to pyruvate, which then contributes to the TCA cycle via pyruvate dehydrogenase (not shown in schematic) and to mitochondrial OAA. Increased TCA cycle flux increases catalysis of succinyl-coenzyme A (Succ-CoA in the figure) to succinate by two nucleotide-specific isoforms of the enzyme SCS. While SCS-ATP produces one ATP per turn of the TCA cycle, SCS-GTP produces one GTP. Mitochondrial GTP (mtGTP) is a more specific signal of TCA cycle flux and glucose availability as only 1 mtGTP is produced per turn of the cycle, unlike ATP that can be generated from various reactions. GTP generated in the mitochondrial matrix cannot exchange with the cytosol and is therefore trapped within the matrix. PEPCK-M can however convert OAA to PEP powered by mtGTP hydrolysis. PEP can then exit the mitochondria via CiC – increased mtGTP synthesis can therefore increase PEP synthesis by PEPCK-M and subsequent PEP transport into the cytosol. Once in the cytosol, PEP is catalyzed to pyruvate by PK, causing a relatively high drop in standard free energy equivalent to 2 ATP molecules and larger than that of any other phosphorylated metabolite. The mtGTP cycle, driven by enhanced TCA cycle flux from increased glucose oxidation, and coupled to a large delta in cytosolic free energy via PEP hydrolysis, can potentiate insulin secretion via K^+-ATP channel closure, depolarizing the membrane and triggering Ca^{2+} influx. Notably, mtGTP can allosterically inhibit GDH – however this inhibitory effect is superseded by allosteric activation of GDH by leucine. In collaboration with glutaminase and ASAT, GDH mediates glutamine-stimulated insulin secretion.

Abbreviations: GLUT2, GLUcose Transporter 2; 2-PG, 2-phosphoglycerate; PEP, phosphoenolpyruvate; PK, pyruvate kinase; ATP, 5'-adenosine triphosphate; ADP, 2'-adenosine diphosphate; OAA, oxaloacetate; TCA cycle, Tricarboxylic acid cycle; αKG, α-ketoglutarate; SCS, succinyl coenzyme A synthetase; GTP, 5'-guanosine triphosphate; GDP, 5'-guanosine diphosphate; PEPCK-M, mitochondrial phosphoenolpyruvate carboxykinase; CiC, citrate/isocitrate carrier; SN1, system N1 glutamine transporter; GDH, glutamate dehydrogenase; NADP+, nicotinamide adenine dinucleotide phosphate (oxidized); NADPH, nicotinamide adenine dinucleotide phosphate (reduced); NH_4^+, ammonium ion; ASAT, aspartate aminotransferase.

(B, C) Expression levels of hSCS-ATP or –GTP β-subunit mRNA in INS-1 cells transiently transfected with either the hSCS-ATP or -GTP overexpressing vectors. (n = 3 per group)

(D) Expression level of rat SCSα subunit mRNA in INS-1 cells transiently transfected with either the hSCS-ATP or -GTP overexpressing vectors. (n = 3 per group)

(E) Immunofluorescence and immunostaining of INS-1 cells transiently transfected with either the hSCS-ATP or -GTP overexpressing vectors. Both hSCS-GTP and –ATP are tagged with GFP protein, shown in the left column. TMRE stain shown in the center column shows localization of mitochondria. Merged images of the GFP and TMRE images are shown in the right column, and yellow regions indicate co-localization of mitochondria and GFP-tagged protein. Scale Bar = 10 μm.

(F) SCS-ATP (blue bars) and SCS-GTP (red bars) enzymatic activity in control INS-1 cells and INS-1 cells transfected with mitoGFP, hSCS-ATP or -GTP overexpression constructs. ATP- and GTP-specific SCS activities are the combined activity of human and rat. Enzyme activity is expressed as a percentage of total SCS activity in that group. Total SCS activity (100%) is the combined activity of hSCS-ATP, hSCS-GTP, rat SCS-ATP and rat SCS-GTP. Significance was calculated comparing nucleotide-specific activity in each group to that activity in the control group. (For SCS-ATP activity: INS-1, hSCS-ATP, hSCS-GTP n = 6 per group, MitoGFP n = 5; for SCS-GTP activity: INS-1 and hSCS-GTP n = 6 per group; MitoGFP and hSCS-ATP n = 5 per group).

Data are mean ± SEM. Significance is **P < 0.01, ***P < 0.001, NS = not significant by one-way ANOVA with Dunnett's multiple comparisons test (B-D) and two-way ANOVA with Sidak's multiple comparisons test (F).

Figure S2. Constitutive and inducible expression of hSCS-ATP and hSCS-GTP in INS-1 832/13 cells, Related to Figure 1

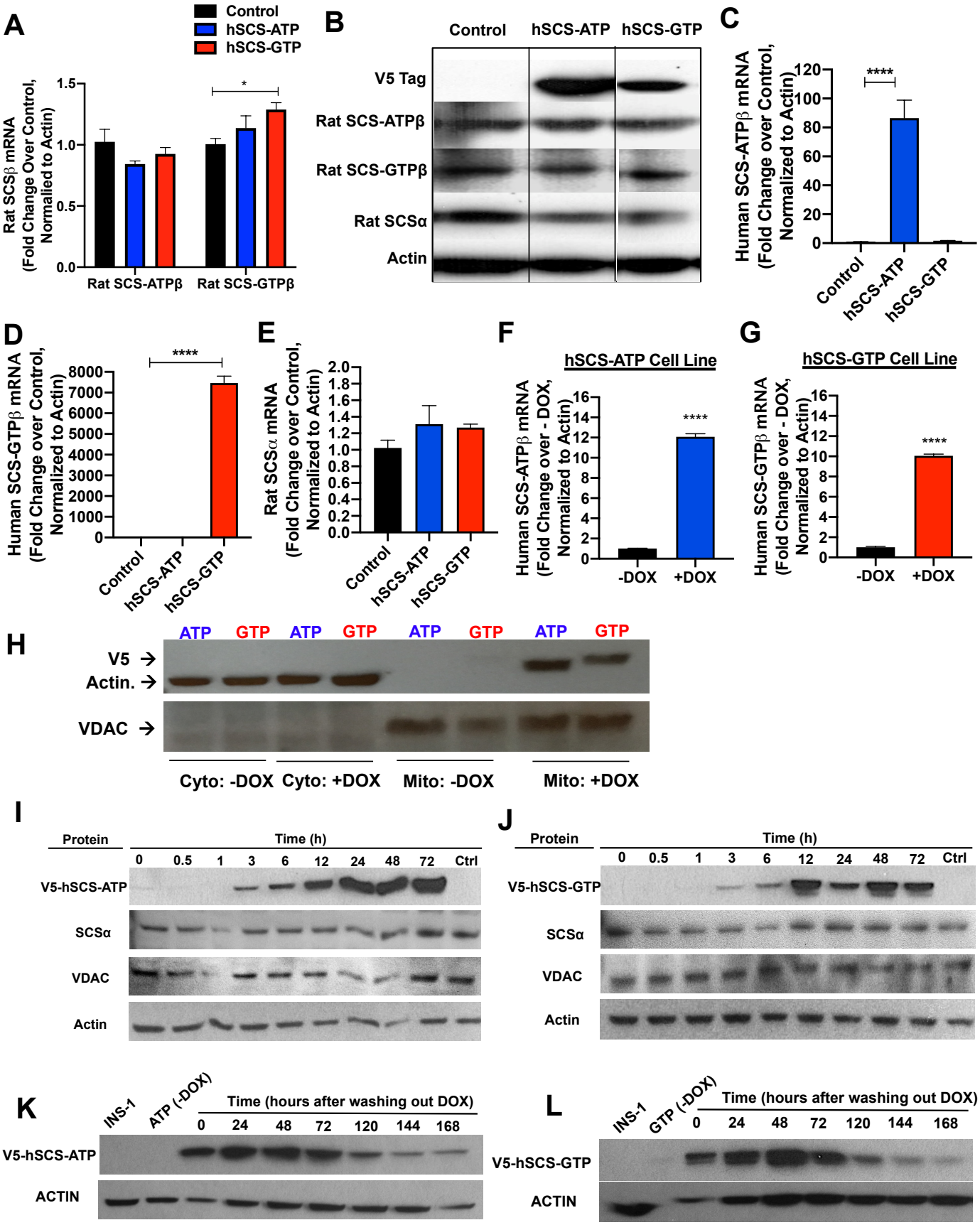

Figure S2. (A) Expression level of rat SCS-ATP or –GTP β-subunits normalized to actin and expressed as fold change over control in control and constitutively overexpressing INS-1 cell lines. (n = 6 per group)
(B) Western blot of V5-tagged hSCS-ATP or -GTP expressed from the transgene in the constitutively overexpressing INS-1 clonal cell lines, and of native rat SCS-ATP, SCS-GTP and SCSα proteins with actin loading control.
(C, D) Expression level of hSCS-ATP and hSCS-GTP β-subunit mRNA in control and constitutively overexpressing INS-1 cell lines. (n = 6 per group)
(**E**) Expression level of rat SCSα subunit mRNA in control and constitutively overexpressing INS-1 cell lines. (n = 6 per group)
(F, G) Expression of hSCS-ATP and -GTP β-subunit mRNA in the inducible cell lines treated with (+ DOX) or without (- DOX) 0.2 μg/mL doxycycline for 48 hrs. (n = 3 per group)
(H) Western blot of V5-tagged hSCS-ATP or hSCS-GTP protein expression in cytosolic (Cyto) and mitochondrial (Mito) fractions from hSCS-ATP and hSCS-GTP inducible cell lines with or without 0.2 μg/mL doxycycline treatment (ATP = hSCS-ATP and GTP = hSCS-GTP). Actin is the loading control for cytosolic fractions and VDAC is the loading control for mitochondrial fractions.
(**I, J**) Western blots showing time-dependent changes in protein expression of V5-tagged hSCS-ATP or hSCS-GTP, native rat SCSα, VDAC and actin after exposure to 0.2 μg/mL doxycycline treatment.
(**K, L**) Western blots showing time-dependent changes in protein expression of V5-tagged hSCS-ATP or hSCS-GTP and actin after removal of DOX from media (washing out of DOX).
Data are mean ± SEM. Significance is *P < 0.05, ****P < 0.0001 by two-way ANOVA with Sidak's multiple comparisons test (A), one-way ANOVA with Dunnett's multiple comparisons test (C-E), and unpaired two-tailed t-test (F, G).

Figure S3. Phenotype of Pre-backcrossed TaBaSCo Mice on Mixed Background (50% B6, 50% CD-1) and Mosaicism in TaBaSCo Islets with Back-Crossing, Related to Figure 2.

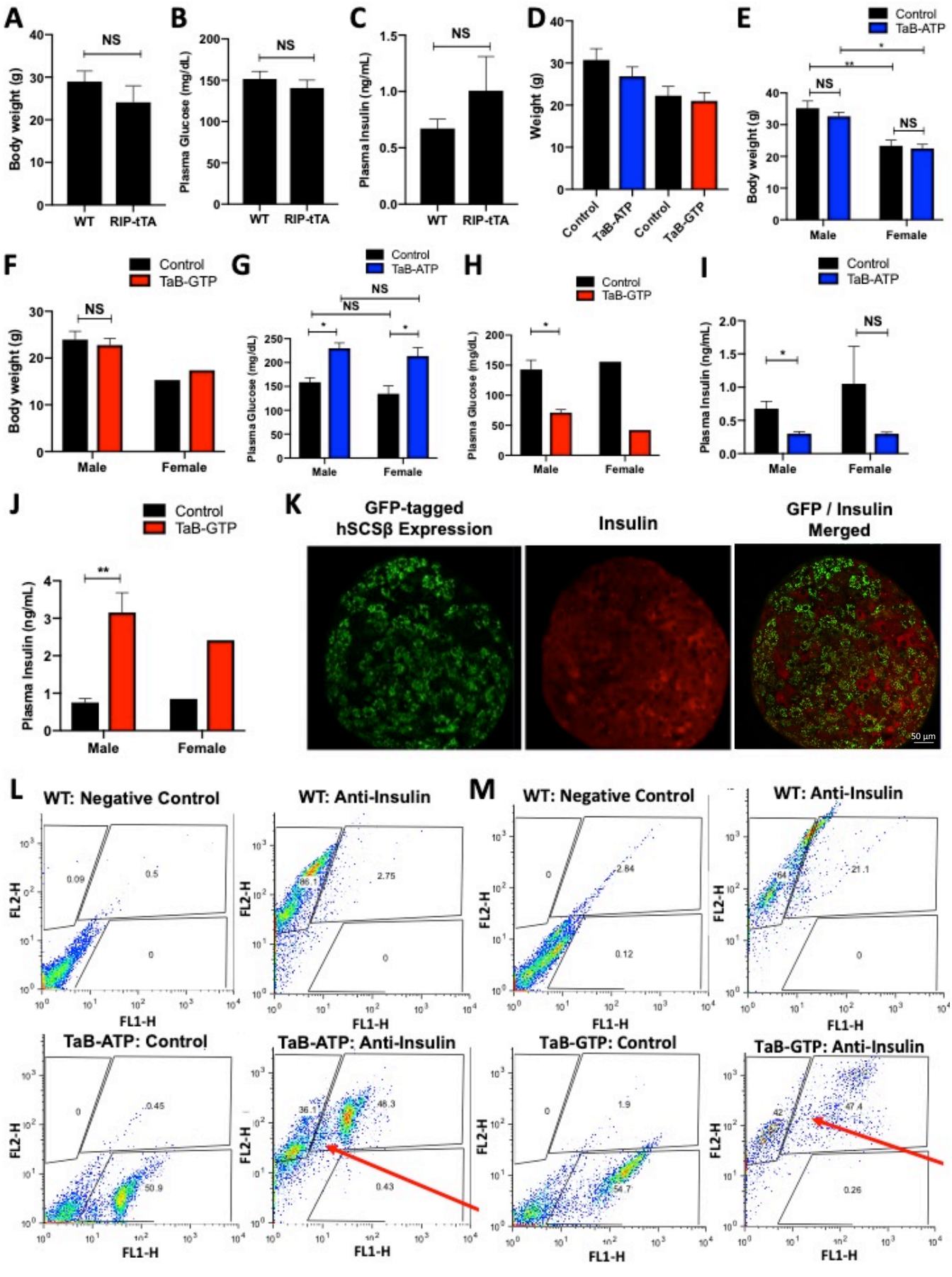

Figure S3.

(A) Body weight (WT: n=9, RIP-tTA: n=4),

(B) Fasting plasma glucose (WT: n=9, RIP-tTA: n=4) and

(C) Fasting plasma insulin in wild-type (WT) mice compared to RIP-tTA mice from crosses with mice carrying the transgene for overexpression of GFP-tagged human SCS β-subunit under regulation of the tet-operon such that transgene is active only with co-expression of RIP-tTA. These WT and RIP-tTA mice do not carry the transgene, and are collectively referred to as the "control" groups shown in the black bars in the following graphs. (WT: n=9, RIP-tTA: n=5)

(D) Body weights of TaBaSCo-ATP (TaB-ATP; blue bar) compared to control littermates, and TaBaSCo-GTP (TaB-GTP; red bar) compared to control littermates. Separate control groups were required since crosses of transgene-carrying mice to RIP-tTA mice were as follows: SCSA x RIP-tTA = TaBaSCo-ATP; SCSG x RIP-tTA = TaBaSCo-G. Therefore, littermate controls for each transgenic mouse are from separate crosses. (Control TaB-ATP: n=8, TaB-ATP: n=7, Control TaB-GTP: n=5, TaB-GTP: n=3)

(E) Body weights of male and female TaB-ATP mice compared to control littermates. (Male Control: n=5, Male TaB-ATP: n=3, Female Control: n=3, Female TaB-ATP: n=4)

(F) Body weights of male and female TaB-GTP mice compared to control littermates. (Male Control: n=4, Male TaB-GTP: n=2, Female Control: n=1, Female TaB-GTP: n=1)

(G) Fasting plasma glucose concentrations in male and female TaB-ATP mice compared to control littermates. (Male Control: n=5, Male TaB-ATP: n=3, Female Control: n=3, Female TaB-ATP: n=4)

(H) Fasting plasma glucose concentrations in male and female TaB-GTP mice compared to control littermates. (Male Control: n=4, Male TaB-GTP: n=2, Female Control: n=1, Female TaB-GTP: n=1)

(I) Fasting plasma insulin concentrations in male and female TaB-ATP mice compared to control littermates. (Male Control: n=6, Male TaB-ATP: n=3, Female Control: n=3, Female TaB-ATP: n=4)

(J) Fasting insulin glucose concentrations in male and female TaB-GTP mice compared to control littermates. (Male Control: n=4, Male TaB-GTP: n=2, Female Control: n=1, Female TaB-GTP: n=1)

(K) Confocal images of whole islets from representative "tet-off" TaBaSCo-GTP mice co-stained with anti-GFP (green, top panel) and anti-insulin (red, middle panel) antibodies. Superposition (bottom panel) shows mosaic expression of the transgene in the insulin positive cells (yellow). Scale Bar = 50 μm.

(L, M) FACS analysis from islets of wild type (WT), TaBaSCo-ATP and TaBaSCo-GTP mice without (left panels) and with (right panels) insulin staining. FL1-H is GFP autofluorescence and FL2-H is anti-insulin staining.

Data points are mean ± SEM. Significance is *P<0.05, **P<0.01, NS= not significant by unpaired two-tailed t-test with Welch's correction (A-C), one-way ANOVA with Tukey's multiple comparisons test (D), two-way ANOVA with Sidak's multiple comparisons test (E, F), two-way ANOVA with Tukey's multiple comparisons test (G) Holm-Sidak unpaired two-tailed t-tests (H, J) and unpaired two-tailed t-test (I).

Figure S4. Fasting Metabolic Profile, glucose homeostasis and insulin secretion in back-crossed TaBaSCo mice and from perifused islets, Related to Figure 2.

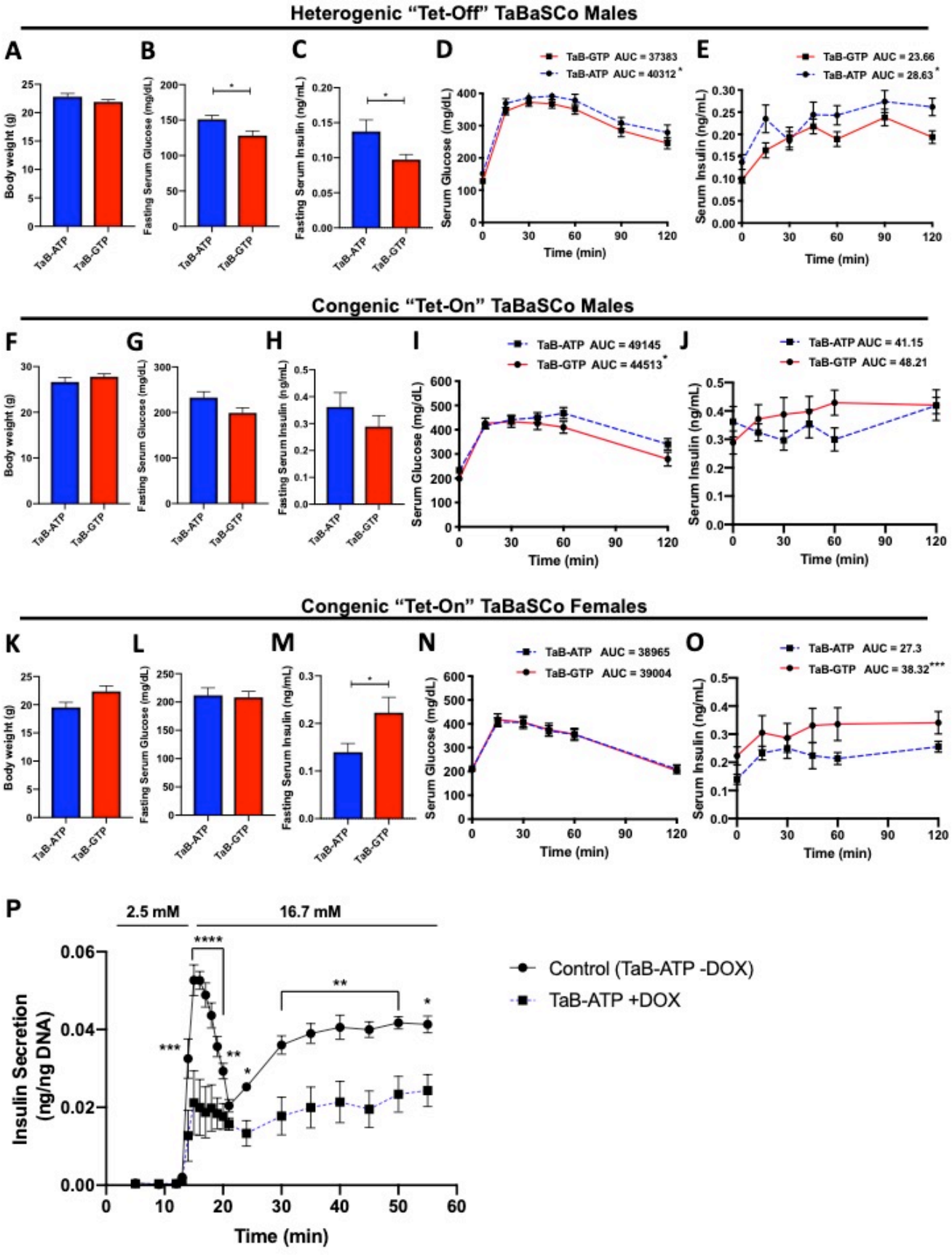

Figure S4. Metabolic profile of backcrossed (to C57BL/6J background at least nine generations) overnight fasted male heterogenic "tet-off" TaBaSCo mice and 6 hour fasted male congenic "tet-on" and female congenic "tet-on" TaBaSCo mice.

Male heterogenic back-crossed "tet-off" mice:

(A) Body weight (TaB-ATP: n = 16, TaG-GTP: n = 17),

(B) fasting serum glucose (TaB-ATP: n = 16, TaG-GTP: n = 18) and

(C) fasting serum insulin concentrations (n = 15 per group).

(D) Serum glucose concentrations measured during a glucose tolerance test (TaB-ATP: n = 16, TaG-GTP: n = 18).

(E) Serum insulin concentrations measured during a glucose tolerance test (TaB-ATP: n = 16, TaG-GTP: n = 17).

Male congenic "tet-on" back-crossed TaBaSCo mice:

(F) Body weight (n = 9 per group),

(G) fasting serum glucose (n = 9 per group) and

(H) fasting serum insulin concentrations (n = 9 per group).

(I) Serum glucose concentrations measured during a glucose tolerance test (n = 9 per group).

(J) Serum insulin concentrations measured during a glucose tolerance test (n = 9 per group).

Female congenic back-crossed "tet -on" mice:

(K) Body weight (TaB-ATP: n = 8, TaG-GTP: n = 11),

(L) fasting serum glucose (TaB-ATP: n = 9, TaG-GTP: n = 11) and

(M) fasting serum insulin concentrations (TaB-ATP: n = 9, TaG-GTP: n = 10).

(N) Serum glucose concentrations measured during a glucose tolerance test (TaB-ATP: n = 9, TaG-GTP: n = 11).

(O) Serum insulin concentrations measured during a glucose tolerance test (TaB-ATP: n = 9, TaG-GTP: n = 11).

(P) Isolated islets from untreated, female tet-on mice were incubated for 24 hours with 0.2 µg/mL doxycycline treatment (+DOX) or vehicle (-DOX), then perifused at basal 2.5 mM glucose followed by stimulatory 16.7 mM glucose, and first and second phase insulin secretion was measured (n = 4 per group).

For all serum glucose and insulin data from the glucose tolerance tests (D, E, I, J, N, O) the calculated areas under the curves (AUC) are indicated in parentheses in the graph legends with corresponding significance marked with asterisks.

Data points are mean ± SEM. Significance is *P<0.05, **P<0.01, ***P<0.001, ****P<0.0001 by unpaired two-tailed t-test with Welch's correction (A, B, K-M), unpaired two-tailed t-test (C, F-H), Holm-Sidak unpaired two-tailed t-test (D, E, I, O, P), Wilcoxon matched pairs rank test (J, N) and paired two-tailed t-test (O).

Figure S5. Morphological characteristics of insulin granules in INS-832/13, hSCS-ATP and hSCS-GTP cells determined by TEM, Related to Figure 4.

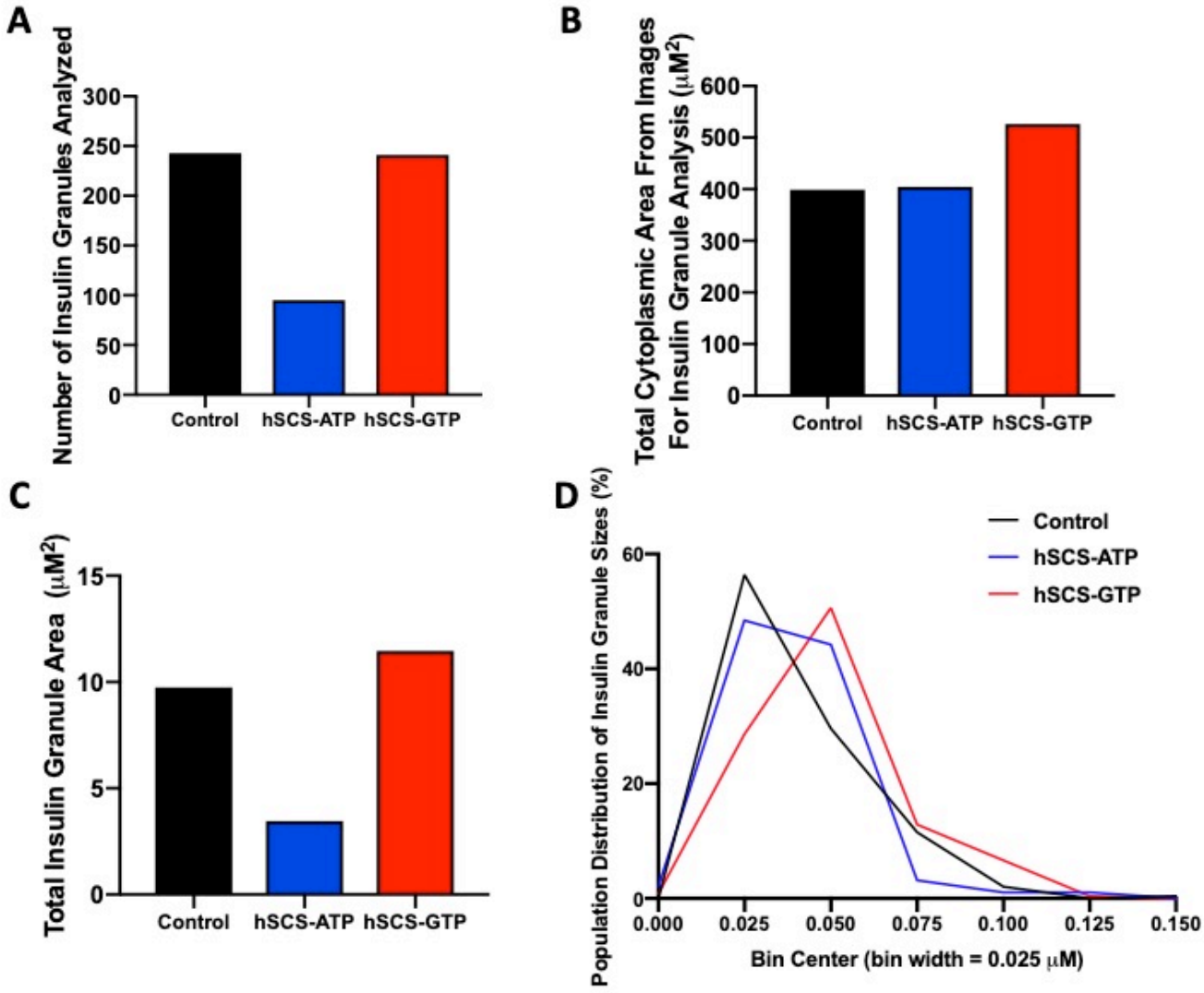

Figure S5.

(A) Total number of insulin granules analyzed in the TEM images for each cell line.

(B) The total cytoplasmic area, per cell line, calculated from TEM images that contained insulin granules.

(C) The total insulin granule area, per cell line, calculated from TEM images that contained insulin granules.

(D) Population distribution of insulin granules in each cell line from Figure 4G. Shown as relative frequency, bin size 0.025μm.

Figure S6. Metabolic characterization of INS-1 832/13, hSCS-ATP and hSCS-GTP cells, Related to Figure 6.

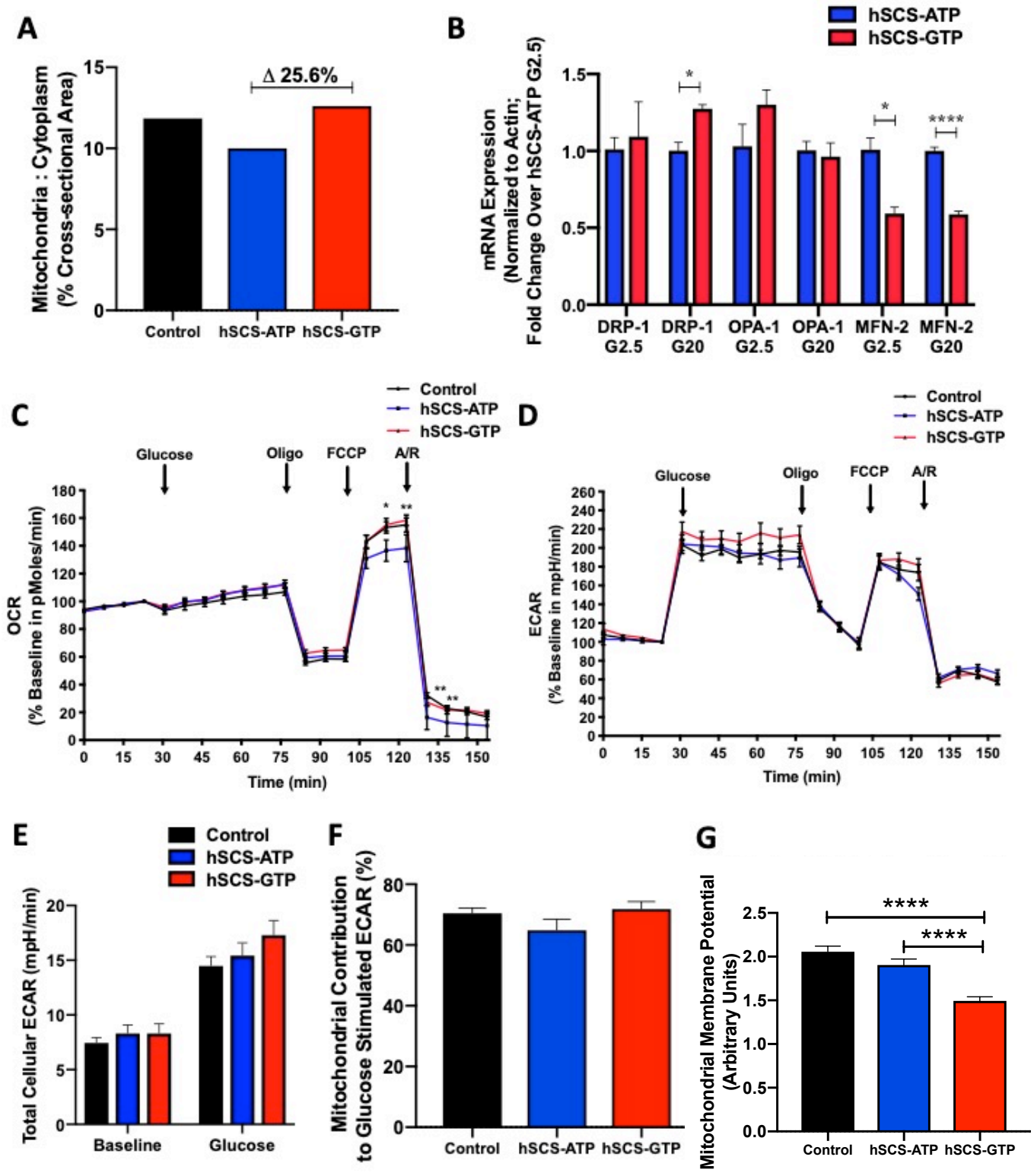

Figure S6.

Ratio of the mitochondrial to cytoplasmic area measured from TEM images of control, hSCS-ATP and hSCS-GTP cell lines

(A) Expression level of mRNA transcripts of mitochondrial fission and fusion markers in hSCS-ATP and hSCS-GTP constitutive cell lines incubated overnight with low 2.5 mM glucose and high glucose (20 mM). Expression was normalized to actin and expressed as fold change over hSCS-ATP. (n=4 per group)

(B) Mitochondrial oxygen consumption rate (OCR; n=8 per group) and

(D) extracellular acidification rate (ECAR) under basal conditions (2.5 mM glucose) and after exposure to 16.7 mM glucose (Glucose), oligomycin (Oligo), FCCP, and antimycin/rotenone (A/R) in control, hSCS-ATP and hSCS-GTP cells (Control, hSCS-GTP n = 8 per group; hSCS-ATP n=7).

(E) Total cellular ECAR at basal and stimulatory glucose from control (n=8), hSCS-ATP (n=7) and hSCS-GTP cells (n=8).

(F) Percentage of mitochondrial contribution to ECAR under basal conditions and after exposure to 16.7 mM glucose in control, hSCS-ATP and hSCS-GTP cells

%Mitochondrial $ECAR_{glucose}$= (100*($ECAR_{glucose}$-ECAR $OCR_{antimycin/rotenone}$/ $ECAR_{glucose}$)) (Control, hSCS-GTP n = 8 per group; hSCS-ATP n=7).

(G) The mitochondrial membrane potential as determined by the ratio of the fluorescence intensity of TMRE/MTG dyes (red/green) which corresponds to the extent of mitochondrial membrane polarization. Control is the INS-1 832/13 parental cell line.

Data are mean ± SEM. Significance is *P < 0.05, ****P<0.0001 by two-way ANOVA with two-stage linear step-up procedure of Benjamini, Krieger and Yekutieli for multiple comparisons (B), two-way ANOVA with Dunnett's multiple comparisons test (B,C), two-way ANOVA with Tukey's multiple comparisons test (E) and one-way ANOVA (F, G).

Figure S7. Steady-State Metabolite Concentrations, Enrichments and ^{13}C-labeled metabolic time-courses measured in hSCS-ATP and hSCS-GTP cell lines, Related to Figure 7.

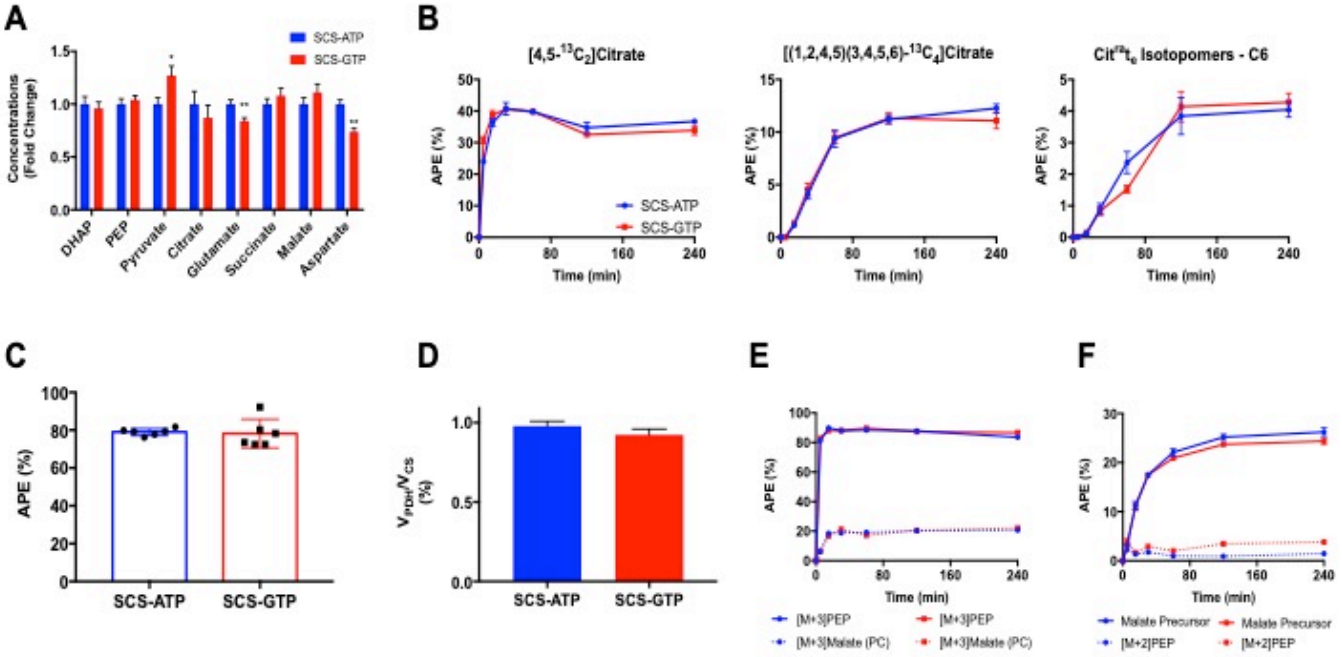

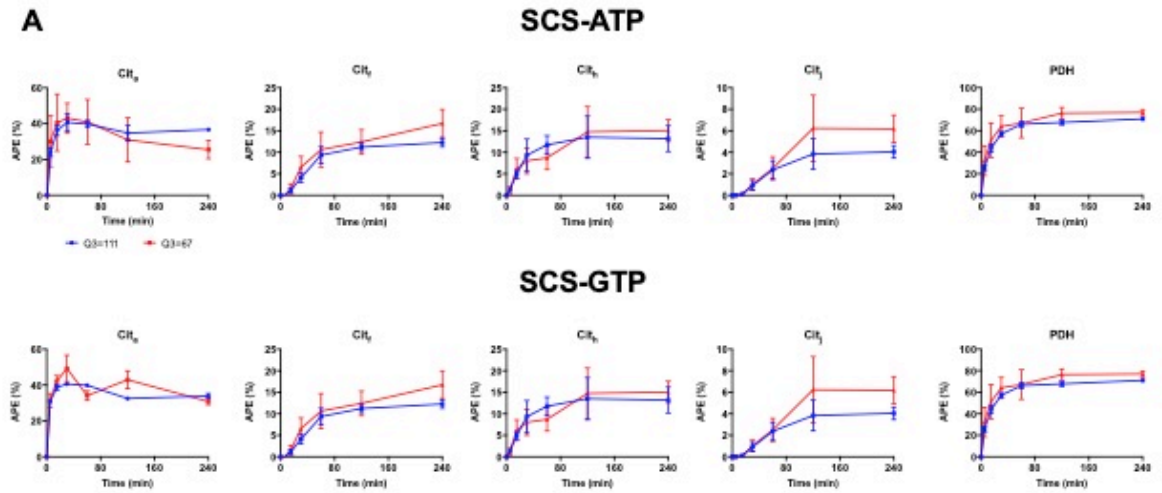

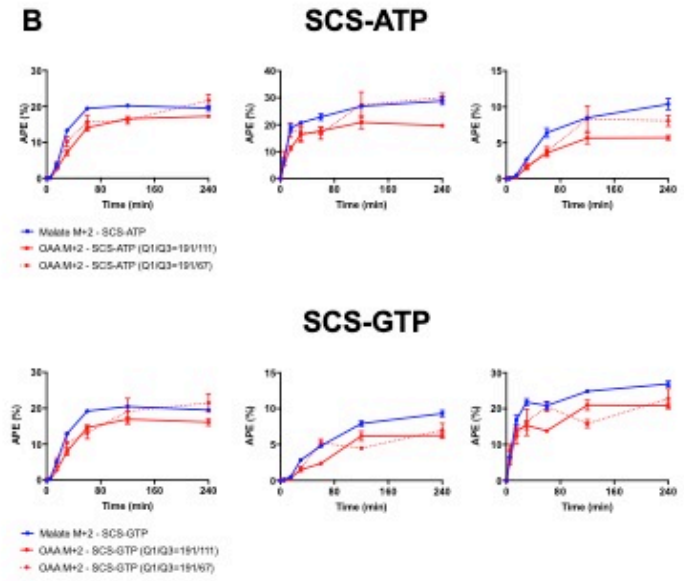

Figure S7.

(A) Concentrations of the metabolites normalized to endogenous taurine.

(B) Time course of ^{13}C-accumulation for isotopomer families generated during different turns of the TCA cycle. The overlapping time courses supported similar V_{CS} in both cell lines.

(C) Steady-state enrichments of [1,2-$^{13}C_2$]acetyl-CoA calculated from the citrate isotopomer analysis. Data is shown as average ± standard deviation.

(D) V_{PDH}/V_{CS} using the results from the mathematical simulation. Data are least-square fit ± standard deviation of the distribution obtained from the Monte-Carlo simulations (n=100). Statistical analysis was performed using an in-built tool in CWave.

(E) Time courses of ^{13}C-enrichment for the precursor ([M+3]PEP) and product ([M+3]Malate(PC)) for SCS-ATP (blue) and SCS-GTP (red). The overlapping time courses supported similar V_{PC} in both cell lines.

(F) Time courses of ^{13}C-enrichment for the precursor (Malate) and product ([M+2]PEP) for SCS-ATP (blue) and SCS-GTP (red). The higher enrichments of [M+2]PEP relative to its precursor support a higher V_{PCK} in the SCS-GTP cell lines.

(G, H) Comparison of all citrate families used as target data in flux modeling using the MRM Q1/Q3=191/111 or Q1/Q3=191/67.

(I, J) Comparison of OAA enrichments calculated from the analysis of Q1/Q3=191/111 or Q1/Q3=191/67 and the measured malate enrichments.

Data is shown as average ± standard error unless otherwise specified. Significance was calculated by a two-tailed, unpaired Student's *t* test, * $P < 0.05$,** $P < 0.005$.

Table S1. List of RT-qPCR Primer Sequences, Related to STAR Methods, Method Details, RT-qPCR

Primer Name	Primer Sequence
b-ACTIN Rat FWD	CCAGATCATGTTTGAGACCTTC
b-ACTIN Rat REV	CATGAGGTAGTCTGTCAGGTCC
SCS-alpha FWD	TGG AGC ATG CCA GAA AGA AT
SCS-alpha REV	GTG TAA GAC CCG TGC CGT AT
Rat SCSATP FWD	AGC CAC CGG TCG CAG ACT ACA
Rat SCSATP REV	TTT GGG GAC AGA GAC GCC CG
Rat SCSGTP FWD	CGG TCA GGT CCC AGG CAG GT
Rat SCSGTP REV	GCC TCC TTA GCA GTG CTG GCG
Human SCSGTP FWD	GAC CGG TCC TGC AAT GGC CC
Human SCSGTP REV	GCC ATC CGC TGA GCT TGG CT
Human SCSATP FWD	CTG TCG CCT GTG CGC CTG C
Human SCSATP REV	CGG TGG TTC CGA AGG GTG GC
GFP FWD	ATC GCC CTG ATA GAC GGT TT
GFP REV	GGG TTG AGT GTT GTT CCA GTT
GGC1 FWD	TCG TGA TCA TTT CAG CGA AC
GGC1 REV	CAG CGG CAA AAG AAC AAT TT
PEPCK-M FWD	TTA TGC ACG ATC CCT TTG CCA TGC
PEPCK-M REV	TCC TTC CTT TGG TAC GAG CCC AAT
PDX-1 FWD	TGC TAA TCC CCC TGC GTG CCT GTA
PDX-1 REV	CTC CTC CGG TTC TGC TGC GTA TGC
FOXO1 FWD	GTG AAC ACC ATG CCT CAC
FOXO1 REV	CAC AGT CCA AGC GCT CAA
Nkx6.1 FWD	TCT TCT GGC CTG GGG TGA TG
Nkx6.1 REV	GGC TGC GTG CTT CTT TCT CCA
DRP-1 FWD	CAG GAA CTG TTA CGG TTC CCT AA
DRP-1 REV	CCT GAA TTA ACT TGT CTC GCG A
OPA-1 FWD	TGA CAA ACT TAA GGA GGC TGT G
OPA-1 REV	CGT TGT GCT GGA TGA CCC TCA A
MFN-2 FWD	AGC GTC CTC TCC CTC TGA CA
MFN-2 REV	TTC CAC ACC ACT CCT CCG AC
Insulin1 rat FWD	CTG CCC AGG CTT TTG TCA A
Insulin1 rat REV	TCC CCA CAC ACC AGG TAC AGA
Insulin 2 FWD	CAG CAC CTT TGT GGT TCT CA
Insulin 2 REV	CAG TGC CAA GGT CTG AAG GT

MafA Rat FWD	TCC AGG CTG GTG CGC GAA AG
MafA Rat REV	GCA AGC CCA CTC AGG AGC CG
Lmyc Rat FWD	GAA GGT GCA TCC GTA CCA CT
Lmyc Rat REV	TCT GGG GAA TAG CCT TGA TG
PC FWD	AGA TGC ACT TCC ATC CCA AG
PC REV	CCT TGG TCA CGT GAA CCT TT
M1/M2-PK FWD	TGG AGA GCA TGA TCA AGA AGC
M2-PK REV	CAC TGC AGC ACT TGA AGG AG
Glucagon rat FWD	GCC GAG GAA GGC GAG ACT
Glucagon rat REV	CAT GTC TGC GCC CAA GTT C
MafB Rat FWD	GAA GCC CGC GAG GCA TAT
MafB RatREV	GGC CCT GGC ACT CAC AAA
ACACA Rat FWD	CGCTCACCAACAGTAAGGTGG
ACACA Rat REV	GCTTGGCAGGGAGTTCCTC

Table S1. Complete sequences for all RT-qPCR primers have been listed in this table. For the RT-qPCR data for which these primers were used, please refer to Figure S1B-D; Figure S2A, C-G; Figure 3A,B,H-J; Figure 4B; Figure 5B-F, H; and Figure S6B.

Table S2. MRM transition pairs (Q_1/Q_3) for all metabolites studied, Related to STAR Methods, Method Details, LC-MS/MS Analysis

Metabolite	Isotopologue	Q_1/Q_3
Citrate	M+0	191/111
	M+1	192/111
		192/112
	M+2	193/112
		193/113
	M+3	194/113
		194/114
	M+4	195/114
		195/115
	M+5	196/115
		196/116
	M+6	197/116
	M+0	191/67
	M+1	192/67
		192/68
	M+2	193/67
		193/68
		193/69
	M+3	194/68
		194/69
		194/70
	M+4	195/69
		195/70
		195/71
	M+5	196/70
		196/71
	M+6	197/71
Succinate	M+0	117/73
	M+1	118/73
		118/74
	M+2	119/74
		119/75
	M+3	120/75
		120/76
	M+4	121/76
Malate	M+0	133/133
	M+1	133/115
	M+2	134/116
	M+3	135/117
	M+4	136/118
Glutamate	M+0	146/41
	M+1	147/41
		147/42
	M+2	148/41
		148/42
		148/43

	M+3	149/41
		149/42
		149/43
	M+4	150/42
		150/43
	M+5	151/43
	M+0	146/128
	M+1	147/129
	M+2	148/130
	M+3	149/131
	M+4	150/132
	M+5	151/133
Pyruvate	**M+0**	87/87
	M+1	88/88
	M+2	89/89
	M+3	90/90
Aspartate	**M+0**	132/115
	M+1	133/116
	M+2	134/117
	M+3	135/118
	M+4	136/119
DHAP	**M+0**	169/97
	M+1	170/97
	M+2	171/97
	M+3	172/97
PEP	**M+0**	167/79
	M+1	168/79
	M+2	169/79
	M+3	170/79

Table S2. Complete list of individual MRM transition pairs (Q_1/Q_3) used for LC-MS/MS metabolite measurement and for ^{13}C-isotopomer analysis (STAR Methods). See Figure 7 and Figure S7.